Chapter 6

Practical Design of Green Catalysts for PET Recycling and Energy Conversion

Arvin Sangalang, Seunghwan Seok and Do Hyun Kim

Additional information is available at the end of the chapter

http://dx.doi.org/10.5772/62041

Abstract

The recycling of chemicals and generation of alternative energy are central topics in the efforts toward sustainable development. Among these, research on plastics recycling and fuel cells has received significant attention, with the aim of designing novel catalysts to improve yield and efficiency. We highlight our work on these areas focusing on the chemical depolymerization of polyethylene terephthalate (PET) to recover its constituent monomer and the development of high-performance anode catalysts for polymer electrolyte membrane fuel cells (PEMFC). We demonstrate various flexible yet practical synthesis strategies (e.g. ultrasound-assisted deposition and biopolymer coating) that were used to obtain catalytic properties optimized for these applications. The effectiveness and simplicity of these methods render the catalysts to be truly green — from synthesis up to process application.

Keywords: PET glycolysis, fuel cell, ultrasound, polydopamine, nanocomposites

1. Introduction

Depleting resources and waste management are the major driving factors for environmental conservation practices, such as recycling and development of alternative energy. Plastics recycling and generation of renewable energy, in particular, are among the direct approaches that aim to curb the consumption of oil-derived commodities. Research efforts on these areas can contribute to the realization of long-term environmental sustainability, aiming for increased productivities and minimal environmental impact. In these efforts, the development of effective catalysts to improve their performance remains a major goal in optimizing processes for resource conservation. Taking both catalytic activity and practical synthesis into account, we present catalyst design strategies that truly conform to principles of green catalysis.

1.1. Chemical recycling of poly(ethylene terephthalate)

Poly(ethylene terephthalate) or PET is currently the world's most widely recycled plastic. Due to its extensive use in various applications, largely in packaging, its worldwide consumption has increased tremendously, adding to the generation of plastic solid wastes. The global market for PET packaging was worth $48.1 billion in 2014, equivalent to about 16 million tons of PET. Furthermore, the projected demand for PET packaging material is estimated to increase further by 4.6% annually, reaching up to 20 million tons by 2019 [1]. The dramatic increase in PET consumption over the past decades has led to significant efforts to recycle the thermoplastic polyester.

The case of PET recycling is currently a logistically well-established, large-scale recycling industry. Bottle recollection rates, for example, have shown a steady increase worldwide, which accounted for at least 2.8 million tons of collected bottles in 2008 (Figure 1). Most of recycled PET flakes produced worldwide are utilized for fiber applications. PET recycling, at present, is largely dominated by physical methods or melt-phase recycling strategies, although various process routes have been studied and remain open to major advancements for better sustainability [2–4].

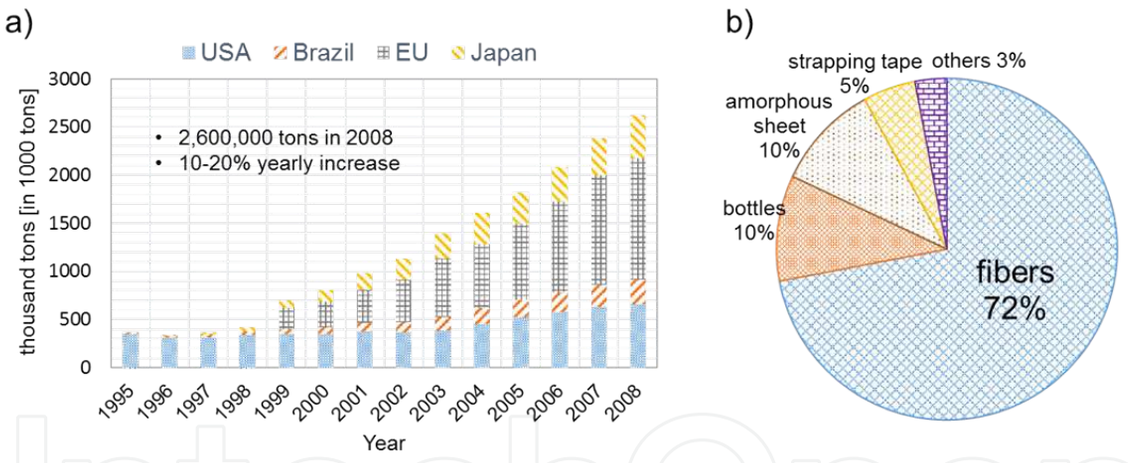

Figure 1. a) Increase in PET bottle recollection rates in various regions worldwide from 1995 to 2008. b) Use distribution of recycled PET flakes.

Significant efforts and renewed interest in chemical recycling routes have resurfaced recently, as stronger calls for long-term sustainability and new process developments in chemical recycling appeared. Extensive reviews on the progress and various aspects of PET chemical recycling are available elsewhere [2–7]. It has been regarded in the recycling literature that chemical recycling offers the most viable approach of sustainable recycling, allowing the recovery of raw materials and other useful chemicals while dealing with long-term waste disposal issues [5]. Figure 2 shows the monomer recovery routes in PET synthesis and chemical recycling. Among them, glycolysis is the simplest and well established, requiring low to moderate process conditions and capital investment (Table 1) [2].

http://dx.doi.org/10.5772/62041

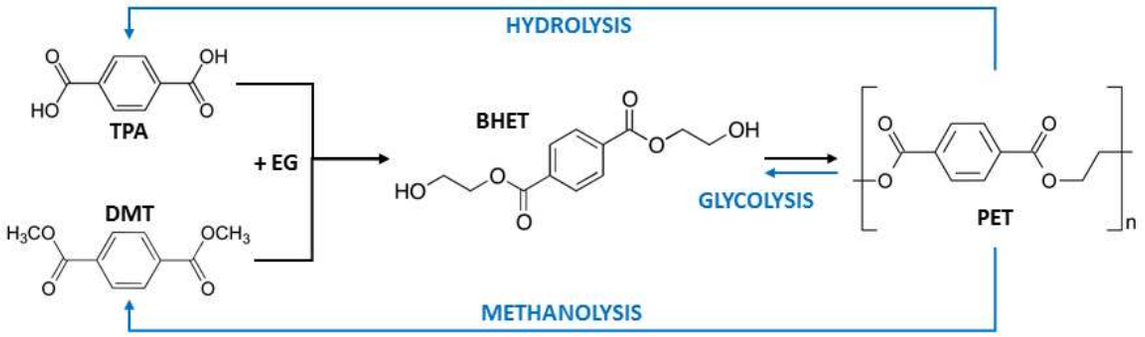

Figure 2. PET monomer recovery routes.

Recycling process	Qualitative plant cost	Economically competitive scale	Safety conditions
Hydrolysis	High	Large plants	High
Methanolysis	High	Large plants	High
Glycolysis	Medium-low	Small plants/batch reactor	Medium

Table 1. Process and economic considerations for PET monomer recovery routes [2]

The products obtained from glycolysis are the polycondensation monomer of PET, bis(2-hydroxyethyl terephthalate) or BHET (Figure 3) and low molecular weight oligomers, which are purified for subsequent use in PET manufacture or conversion into other chemicals. There have been significant issues, however, in process efficiency and product purification that led to recent efforts in the development of novel catalysts.

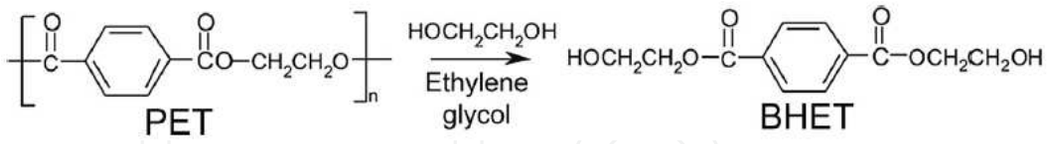

Figure 3. Glycolysis of PET chain releasing the monomer BHET.

Catalyst use is crucial in glycolysis and those used in earlier studies still required long reaction times despite catalyst application. These include metal acetates, alkalis, sulfates, and chlorides, some of which are those of toxic heavy metals [5]. Aside from efficiency, catalyst separation has been a major drawback in these catalysts together with environmental concerns. Despite chemical recycling being touted as the superior viable recycling route in the long-term, significant process developments are needed before it can truly be considered as a practical and competitive alternative to mechanical recycling. Results of life cycle assessments (LCA) show (Figure 4) that not only chemical recycling incurs greater process costs, but it also contributes to an overall negative impact in terms of a larger net consumption of non-renewable energy source and environmental effects [4]. Fortunately, recent developments in

novel catalyst design may offer effective solutions to achieve the goal of a truly green and viable PET chemical recycling.

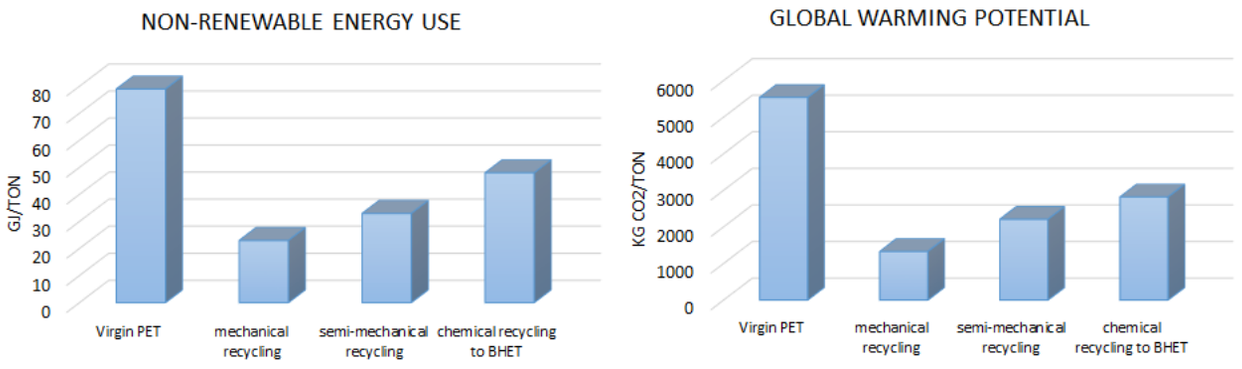

Figure 4. Comparison of life cycle assessment (LCA) results for PET manufacture and recycling in terms of non-renewable energy use and equivalent CO_2 generated per ton of PET fiber [4].

1.2. Hybrid catalysts for polymer electrolyte membrane fuel cells

The development of hybrid catalysts for polymer electrolyte membrane fuel cells (PEMFCs) has received attention recently due to advantageous qualities in its interaction characteristics and physical durability. The combination of conductivity enhancement and water management becomes widely used to improve PEMFC performance without external humidifying system. In this respect, requirements for next promising materials for PEMFCs include such categories as high proton conductivity, membrane electrode assemblies (MEA), and non-toxic and easy fabrication method. The humidifying ability of MEA in fuel cells is crucial for proton conductivity. As such, the approach to enhance conductivity and allow self-humidification at the same time has been considered recently to improve the performance of PEMFCs [8]. Given these requirements, the potential solution is platinum doping for conductivity and using silica as support for its hygroscopic properties. It is a challenge, however, to increase the platinum doping and enhance catalyst conductivity. With our bio-coating strategy for metal doping, we demonstrate a successful implementation of N-doped carbon composite through a silica-based templating technique [9]. In contrast to other reported methods that use chemical vapor deposition (CVD) and plasma treatment of various nitrogen precursors, our method remains on the practical side requiring no expensive equipment and complex treatment processes.

2. Synthesis and performance of metal oxide-based catalysts for PET glycolysis

Clearly, there is a need to consider various factors in designing PET glycolysis catalysts such as catalytic activity, ease of process applicability, and environmental impact. The coordination between a metal cation and the PET carbonyl oxygen is the widely exploited basis of catalytic

http://dx.doi.org/10.5772/62041

activity in glycolysis, although other catalytic pathways do exist. Numerous metal compounds have been used as glycolysis catalysts with varying success [6]. Some of these made its way to commercial application through patented technologies [7]. Recently, a significant amount of work in the development of solid catalysts has appeared, potentially addressing the problem of product/catalyst separation.

The first solid catalysts used for glycolysis were zeolites, which showed catalytic performance of only moderate monomer yields (<70%). We have developed various glycolysis catalysts based on metal oxides that were thermally stable and recoverable and provided excellent monomer recovery yields. These are the ideal characteristics of industrially applicable heterogeneous catalysts that could solve issues in existing conventional glycolysis catalysts. We discuss in the following sections several methods used to synthesize them, their properties, and performance as stable and effective glycolysis catalysts. It was possible to obtain free and supported versions of these catalysts using flexible synthesis strategies [10–13] tailored to specific process applications.

2.1. Glycolysis reaction set-up and product analysis

Virgin PET pellets were obtained, mixed with dry ice in a grinder, and reduced to a fine powder with a particle size of <200 μm. The glycolysis reactions were carried out in a 10-mL stainless steel batch-type pressure reactor at 300°C and 1.1 MPa, unless otherwise specified. The reactant mixture of 0.3 g of PET, 1.1 g of EG, and a set amount of catalyst was loaded into the reactor. The reactor was placed in a furnace preheated at the reaction temperature, which, after the given reaction time, was taken out and quenched in cold water to stop the reaction. For quantitative determination of the monomer yield, the reaction products were dissolved in tetrahydrofuran (THF) and analyzed via HPLC. A reverse-phase Zorbax-C8 column and an ultraviolet (UV) detector set at 254 nm were used. The mobile phase used was a 50:50 (v/v) THF/H_2O solution at a flow rate of 1.0 ml/min. The molar yield of BHET was calculated based on the following equation:

$$\text{BHET Molar yield, \%} = \frac{\text{moles of BHET produced}}{\text{moles of PET units}} \times 100\%$$

The monomer BHET was separated from the glycolysis products and purified for qualitative analysis. Boiling water was added to the reaction mixture to dissolve BHET and the hot solution was immediately filtered. Repeated washing was done to extract residual BHET in the filter cake. The filtrate was stored in a refrigerator at 4°C for 24 h, after which white needle-like crystals formed. These were filtered and dried at 70°C for 12 h. The dried crystals were then used for various characterization steps, such as FT-IR, DSC, TGA, and NMR to verify the structure and properties of the recovered monomer, properly distinguishing BHET from its dimer and/or oligomers. Its chemical structure was analyzed by ^{1}H NMR and ^{13}C NMR using DMSO-d_6 as the solvent [10].

2.2. Supported metal oxide composites via ultrasound-assisted synthesis

Metal oxides find important application as catalysts, but agglomeration during their synthesis reduces the active surface area beneficial for catalysis. The combination of solid support and metal has been proposed, since composite materials can isolate the nanoparticle on the supporting material and effectively reduce its size. As a result, such nanocomposites can increase the surface area of metal oxide catalyst [14–16]. Silica, one of the most widely used catalyst supports, is synthesized in this study in the nanoscale and used as a metal oxide support material. Another material considered as support for nanocomposites is graphene oxide (GO). It is compatible with various organic/inorganic nanomaterials, taking advantage of possible chemical modification utilizing the oxygen-containing functional group on its sheet. In addition, it has high chemical stability and specific surface area [17–20]. The synthesis of silica and graphene oxide-based catalysts is presented, where ultrasound was used to reduce reaction time, simplify reaction steps, or perform synthesis in milder conditions.

2.2.1. Ultrasound-assisted catalyst synthesis

Ultrasound has been used in metal deposition, dish cleaning, chemical reactions, and particle dispersion in a solvent [21]. The cavitation phenomenon includes formation, growth, and collapse of bubbles generated in the aqueous solution under ultrasonic irradiation. The phenomenon causes both high temperature (~5000 K) and pressure (~1000 atm) during the sequence of bubble collapse. In a short span of time for bubble formation, it provides very high heating and cooling rate. This unique condition generates intense energy that converts water into H and OH radicals, promoting the formation of metal nanoparticles [22].

Our group applied the ultrasound irradiation method for the fabrication of metal-doped silica nanocomposites [8,11,23,24]. The acoustic cavitation phenomenon facilitates interparticle collision between metal and support material, inducing the binding between metal and support [25,26]. As a result, metal doped on supporting material can be prepared without surfactants or surface modification of support material in a short reaction time and mild reaction conditions.

2.2.2. Ultrasonic deposition of metal oxide catalyst on silica particles

Silica microparticles (SMPs) and silica nanoparticles (SNPs) were used as support for the catalysts. Silica microparticles with size 1–20 μm were purchased from Junsei Chemicals and used without any treatment. Nanosized silica particles were synthesized using the Stöber method, with some modifications. In a sealed round-bottomed flask, 8.0 ml of ammonium hydroxide (28 wt%) and 6.0 ml of deionized water were added to 100 ml of ethanol and stirred for 15 min. Then, 4.7 ml of the silica precursor tetraethyl orthosilicate (TEOS) were added to this solution and stirred at room temperature for 3 h. The resulting precipitate was centrifuged and washed with water and ethanol several times. The product was dried in an oven at 70°C for 8 h followed by calcination at 500°C for 12 h.

To synthesize the silica-supported manganese oxide or zinc oxide catalysts, a predetermined amount of silica support was added to a 1.0 M solution of the precursor [$Mn(NO_3)_2$ xH_2O or

http://dx.doi.org/10.5772/62041

$Zn(NO_3)_2$ $6H_2O$]. The metal oxide loading was set to be 15 wt%. Using a horn-type sonifier, the solution was sonicated for 45 min. A 0.1 M ammonia solution was added at the start of the sonication step in order to keep the pH at around 9.5. The ultrasound-assisted deposition process is illustrated in Figure 5. After separating the particles by centrifugation, they were washed with water and ethanol. The catalyst samples were then dried at 100°C for 8 h and calcined at 350°C for 3 h.

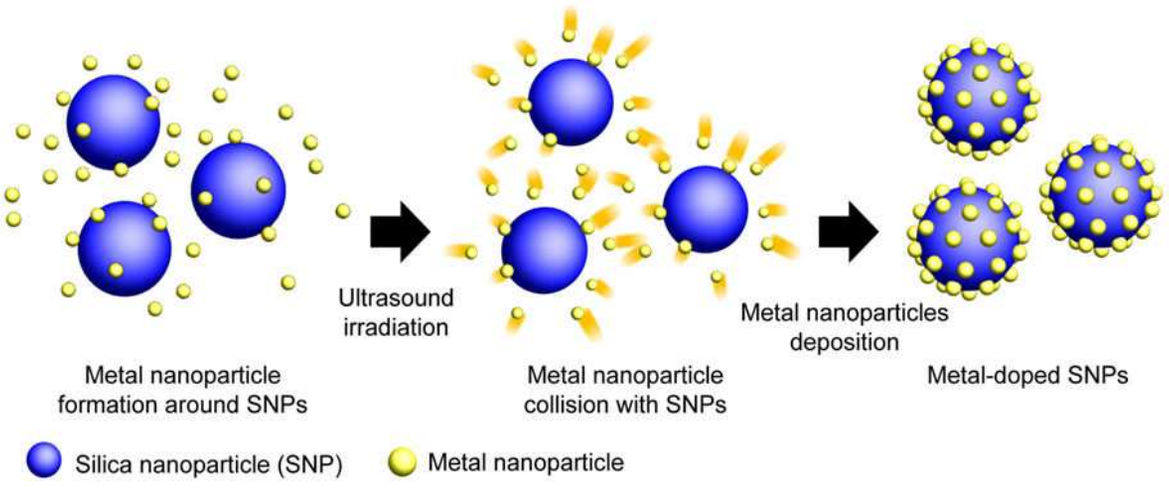

Figure 5. Overall synthesis procedure of metal-doped silica nanoparticle.

The properties of the synthesized silica-supported catalysts are given in Table 2. At 1.0 wt% catalyst-to-PET loading, glycolysis was performed at 300°C for 80 min, after which the product monomer was recovered. Shown in Figure 6 are the FT-IR spectra of the recovered BHET crystals and standard BHET sample. The matching spectra confirm that the product obtained using the silica-supported catalyst was indeed the monomer. The spectrum showed the presence of peaks corresponding to the functional groups in BHET: an -OH band at 3,424 and 1,128 cm^{-1}, an aromatic C-H at 1,456–1,502 cm^{-1}, C-O at 1,712 cm^{-1}, and alkyl C-H at 2,879 and 2,964 cm^{-1} [10].

From the monomer yield versus reaction time data in Figure 7, the order of catalytic activity can be determined as Mn_3O_4/SNPs>ZnO/SNPs>Mn_3O_4 SMPs>ZnO/SMPs. This trend follows the same order as the catalyst surface area and the pore volume given in Table 1. Among the four catalyst samples with different size of support and metal oxide doping, the large amount of active surfaces in the nanoparticle support and the activity of the Mn_3O_4 catalyst could be responsible for the fastest reaction rate and the maximum monomer yield [10]. Although it is evident that using a silica nanoparticle support could improve the catalytic performance, it also has its drawbacks in the practical and industrial perspective. Using a metal oxide catalyst is desired for easier purification of the glycolysis products, but efficient separation of a nanosized catalyst can be challenging. A trade-off between catalytic performance and practical applicability will be inevitable, unless an effective method to separate the catalysts is provided.

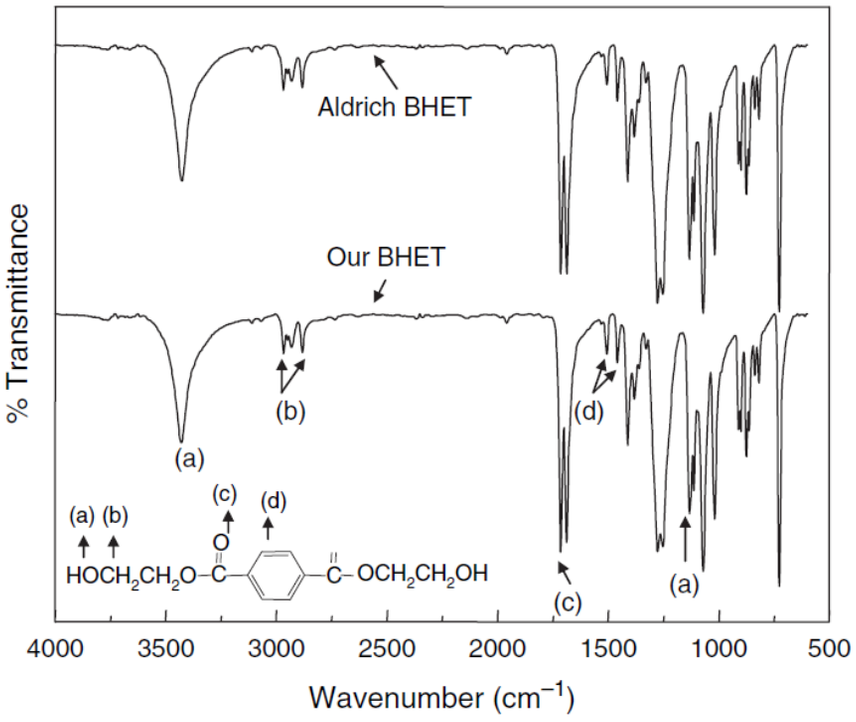

Figure 6. Comparison of FT-IR spectra of standard BHET and BHET recovered from catalyzed glycolysis. Figure from [10].

Catalyst	BET surface area (m^2/g)	Pore volume (cm^3/g)	Average pore diameter (nm)
ZnO/SMPs	2.49	0.014	21.4
Mn_3O_4/SMPs	3.38	0.020	24.4
ZnO/SNPs	22.44	0.154	30.2
Mn_3O_4/SNPs	45.09	0.214	18.9

Table 2. BET surface area, pore volume, and average pore diameter of silica-supported metal oxide catalysts [10]

2.2.3. Sonochemical synthesis of the GO-Mn_3O_4 composites

Mn_3O_4 and its nanocomposites have been utilized as highly effective catalysts for various applications, including PET glycolysis as demonstrated in our previous studies. Some of the known advantages of manganese oxides include excellent catalytic activity, low cost, abundance, and being environmental benign [27–30]. Depending on the oxidation states of manganese, there are several forms of MnO_x (e.g. MnO_2, MnO, Mn_2O_3, and Mn_3O_4), each of which has different applications. Hausmannite (Mn_3O_4), with both Mn^{2+} and Mn^{3+} ions in its crystal structure, has been widely used in catalytic applications. When loaded onto a support to provide a large surface area and prevent aggregation, it could significantly enhance the depolymerization of PET [10].

http://dx.doi.org/10.5772/62041

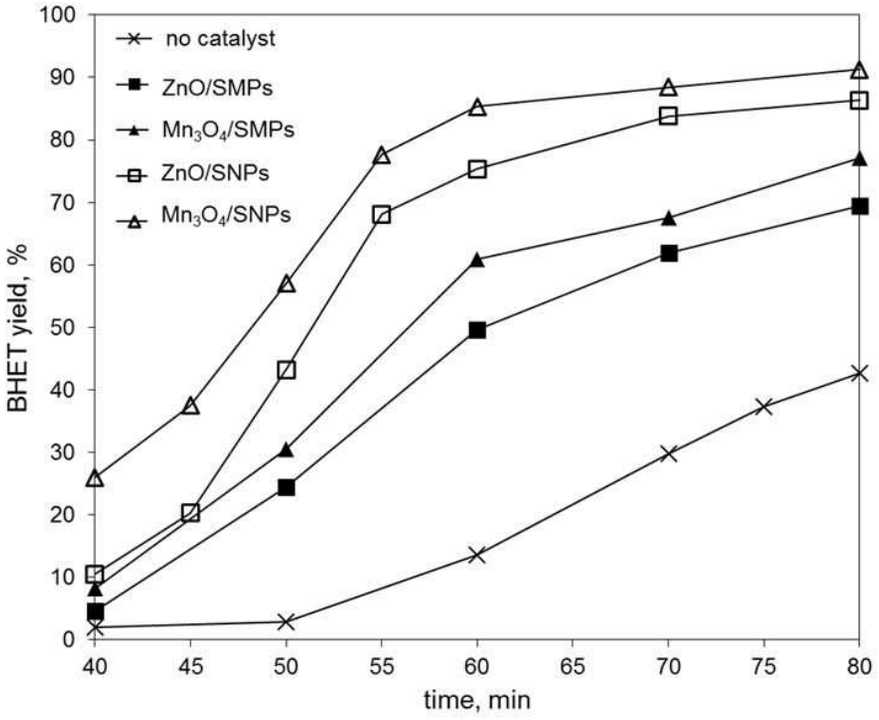

Figure 7. Molar yield of BHET at 300°C and 1.1 MPa using silica-supported catalysts. Figure from [10].

Simultaneous formation and direct deposition of MnO_x nanostructures have been reported by using redox reaction and electrodeposition [21,29–31]. One of the most favorable methods to do this is the reduction of permanganate ions into the insoluble manganese dioxide induced by carbon such as that in a graphene structure. The procedure is simple and the reaction has a self-limiting character [27,28,32]. This method can also be adapted to deposit Mn_3O_4 onto graphene through thermal reduction of MnO_2 over 1000°C [16]. This is an energy-intensive process, over which alternative methods of synthesis using milder conditions would be preferable [21,33]. In our work, sonochemical methods were used to facilitate mild conditions for synthesis and reduce reaction time involved in Mn_3O_4 deposition as illustrated in Figure 8.

Using the modified Hummers method, graphene oxide (GO) was prepared from graphite flakes [34]. One gram of graphite was added to 50 mL of concentrated H_2SO_4 in an ice bath. Then, 3.5 g of $KMnO_4$ were added and stirred for 2 h at 35°C. The suspension was then kept at 98°C to which deionized (DI) water was added dropwise. Then, 25 mL of 3% H_2O_2 aqueous solution were poured into the mixture and filtered with a 0.1 mm pore diameter Anodisc™ membrane. The product was washed with 10% HCl aqueous solution and DI water. By applying ultrasound to the filtered graphite oxide cake suspended in DI water, exfoliated GO was obtained and subsequently dried. Dispersion of GO in DI water at 0.5g/mL concentration was prepared. Mixtures of 10 mg/mL $KMnO_4$ and the GO dispersion at varied volume ratios of 0.01, 0.03, and 0.05 were used for the synthesis of GO-Mn_3O_4 composite samples A, B, and C, respectively. These are then subjected to ultrasonication at a power of 80 W/cm for 30 min using a horn-type sonicator. The resulting suspension was then filtered and washed with DI water and then ethanol [11].

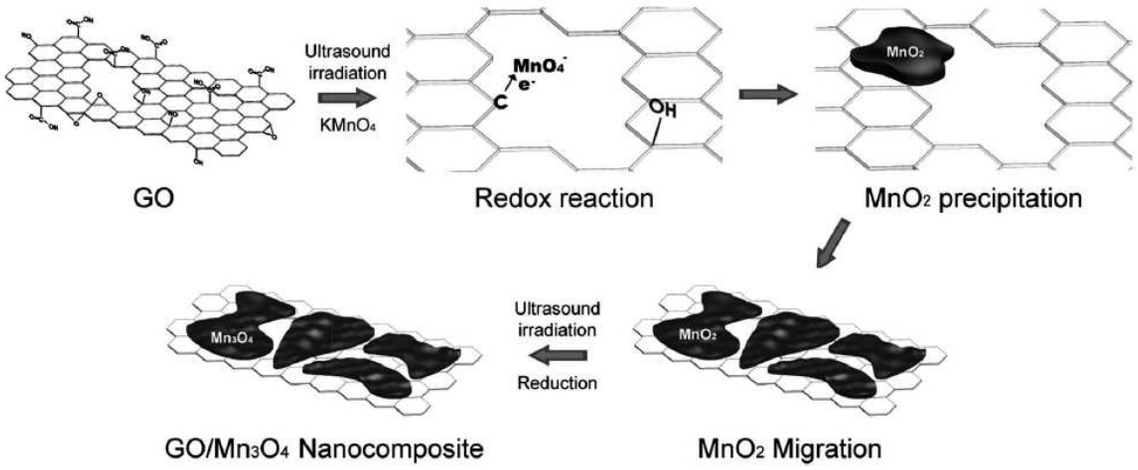

Figure 8. Schematic illustration of ultrasound-assisted synthesis of the GO-Mn_3O_4 composites. MnO_4 is first reduced to MnO_2 and precipitated onto the GO support by oxidizing carbon. The reduction of MnO_2 to Mn_3O_4 then takes place in the following steps.

The formation of GO-Mn_3O_4 nanocomposite was verified by various characterization methods such as XRD, XPS, and Raman spectroscopy. TEM images of pristine GO and the obtained composite are shown in Figures 9a and 9b, indicating the coverage of the GO surface. The high-resolution TEM image in Figure 9c shows the lattice fringes and diffraction pattern of the Mn_3O_4 crystal structure. Compared to the silica-supported composites and conventional metal salt catalysts [10,35], the monomer yield using the GO-Mn_3O_4 nanocomposite was comparable or higher, reaching more than 90% (Figure 10). The yields for the composite were all above 90%, showing improvement from that of bare Mn_3O_4 at 83%. However, the Mn_3O_4 without the support aggregated into micron scale. The GO support could prevent the aggregation of Mn_3O_4 and provide an enlarged and stable active sites [11].

2.3. Magnetically recoverable superparamagnetic γ-Fe_2O_3 nanocatalyst

Efficient recovery of the catalysts in PET glycolysis is an important aspect that several researchers have attempted to address recently. Among the recoverable catalysts studied are various ionic liquids, which were shown to provide molar yields up to 80% [36–39]. Aside from yield, there are several issues that should be considered in using ionic liquids as industrial glycolysis catalysts such as cost, stability, and robustness with respect to process variables such as moisture content, to which ionic liquids are very sensitive [10,11,40]. Urea was also reported to be a reusable glycolysis catalyst at mild temperatures [41]. Vacuum distillation was used to recover the catalyst, however, whose high energy requirements can be counterproductive.

We have studied magnetic nanoparticles as a recoverable glycolysis catalyst, among which γ-Fe_2O_3 was chosen as excellent candidate being known to have good performance in a number of reactions [42–44]. This was the first attempt to utilize magnetic nanomaterials in PET depolymerisation. Nanosized γ-Fe_2O_3 was selected due to its stability, high catalytic activity, and superparamagnetic property [42]. The superparamagnetic behavior allows recovery by application of a magnetic field yet allows good dispersion in the reaction medium, as it has

http://dx.doi.org/10.5772/62041

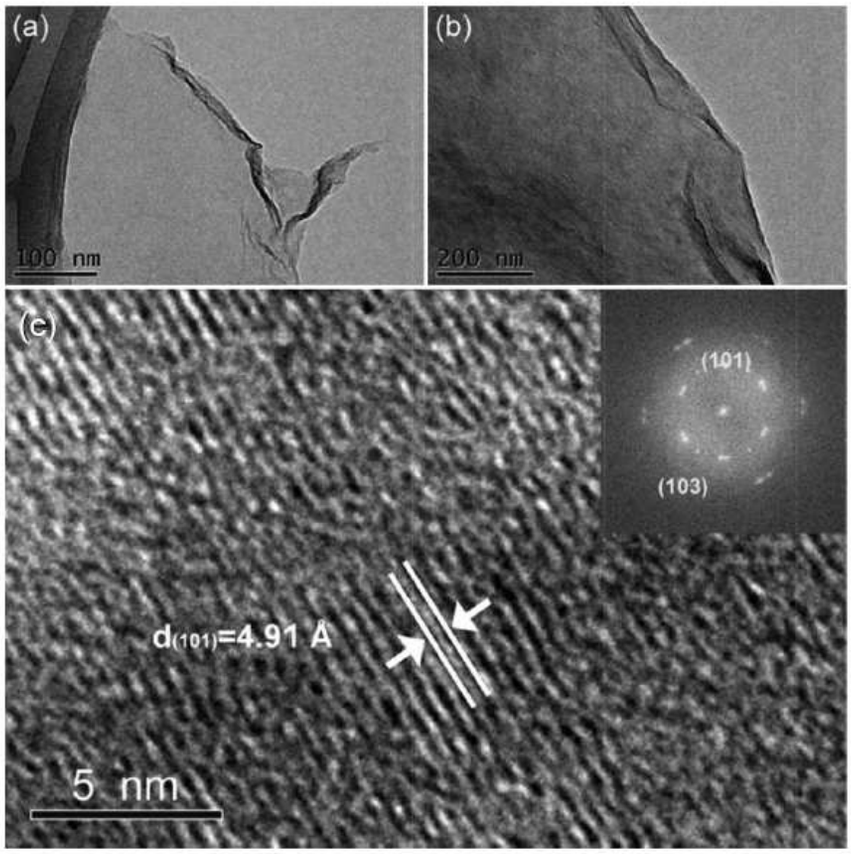

Figure 9. Low-magnification TEM images of (a) GO, (b) GO-Mn_3O_4, and (c) high-resolution TEM image of GO-Mn_3O_4 showing the d-spacing of the (101) crystal plane of Mn_3O_4 and its diffraction rings [11].

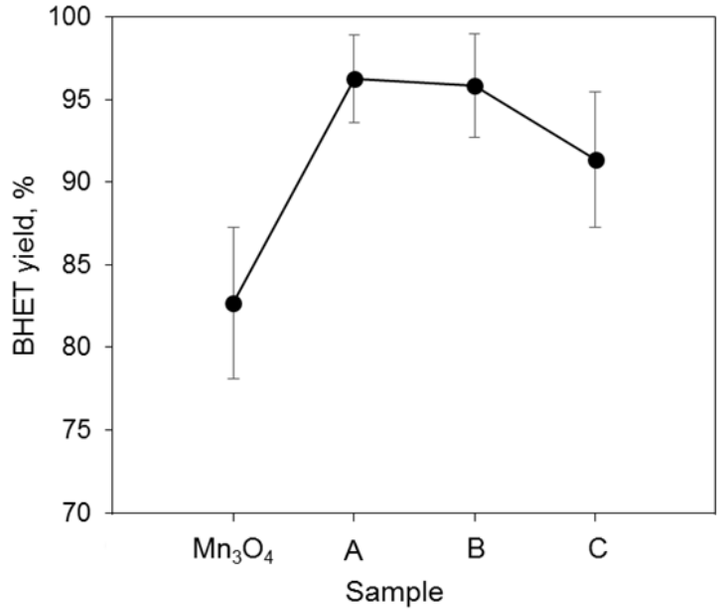

Figure 10. BHET yields for bare Mn_3O_4 and GO-supported Mn_3O_4 catalysts.

zero remanent magnetization. Iron oxides have further advantages being cheap, nontoxic, and abundant [12].

2.3.1. Synthesis of superparamagnetic γ-Fe_2O_3 catalyst and characterization

Slight modifications to the conventional co-precipitation method were done to obtain γ-Fe_2O_3 nanoparticles from Fe_3O_4 [45,46]. For the synthesis of Fe_3O_4 nanoparticles, predetermined amounts of $FeCl_2$ and $FeCl_3$ precursors were dissolved in an HCl solution (0.4 M, 25 mL) to prepare aqueous solutions of Fe^{2+}/Fe^{3+} with 1:2 molar ratio. Sodium hydroxide (1.5 M, 250 mL) was then added rapidly and stirred. The addition of NaOH solution instantly produced a black precipitate, characteristic of Fe_3O_4. The surfactant used to control the particle size was citric acid (0.2 M, 50 mL). The synthesis was performed in a nitrogen atmosphere. The formed black precipitate was separated by placing a magnet and decanting the solution. The product was washed with water four times and centrifuged at 4000 rpm for 4 min. The final washing step was done using a 0.01 M HCl solution in order to neutralize the anionic charges on the nanoparticle surface. Calcination of the dried Fe_3O_4 powder at 210°C for 3 h induced the phase transformation into γ-Fe_2O_3 [12].

The particle morphology of the synthesized catalyst was observed by a 200 kV transmission electron microscope (TEM). As shown in Figure 11a, the particles had a size distribution in the range of 8–14 nm, with mean size of 10 nm. The BET surface area measured was 147 m^2/g. The superparamagnetic property of the nanosized γ-Fe_2O_3 was confirmed by the magnetization curve obtained using a vibrating sample magnetometer (VSM). Figure 11b shows the magnetic behavior in the presence of a magnetic field, exhibiting a strong response with saturation magnetization reaching 47 emu/g. The curve does not have a hysteresis loop and retains no magnetization when the magnetic field is removed. The advantageous consequence of this property is redispersability of the catalyst particles when used in subsequent reactions [12].

The obtained X-ray diffraction (XRD) spectra of the catalyst suggest that the material is γ-Fe_2O_3. This is not conclusive, however, because the XRD patterns of Fe_3O_4 and γ-Fe_2O_3 are very similar. X-ray photoelectron spectroscopy (XPS) analysis of Fe2p cores was performed to distinguish the two phases. Higher binding energies before the calcination as shown in Figure 11c are indicative of Fe_3O_4. The shift to lower binding energies after the calcination step confirms the transformation of Fe_3O_4 to γ-Fe_2O_3 [12].

2.3.2. Catalytic activity, recoverability, and stability with repeated use

The catalytic performance of the synthesized γ-Fe_2O_3 nanoparticles was compared to previously studied silica nanoparticle-supported metal oxide catalysts [10,40]. Under the same reaction conditions and catalyst/PET weight ratio, γ-Fe_2O_3 delivered comparable performance (Figure 12). The BHET yield reached higher than 90% in 70 min at 1.0% catalyst-to-PET loading. As with the supported nanocatalysts, the excellent catalytic performance of the γ-Fe_2O_3 nanoparticles may be attributed to the high surface area and greater accessibility to active sites [12].

http://dx.doi.org/10.5772/62041

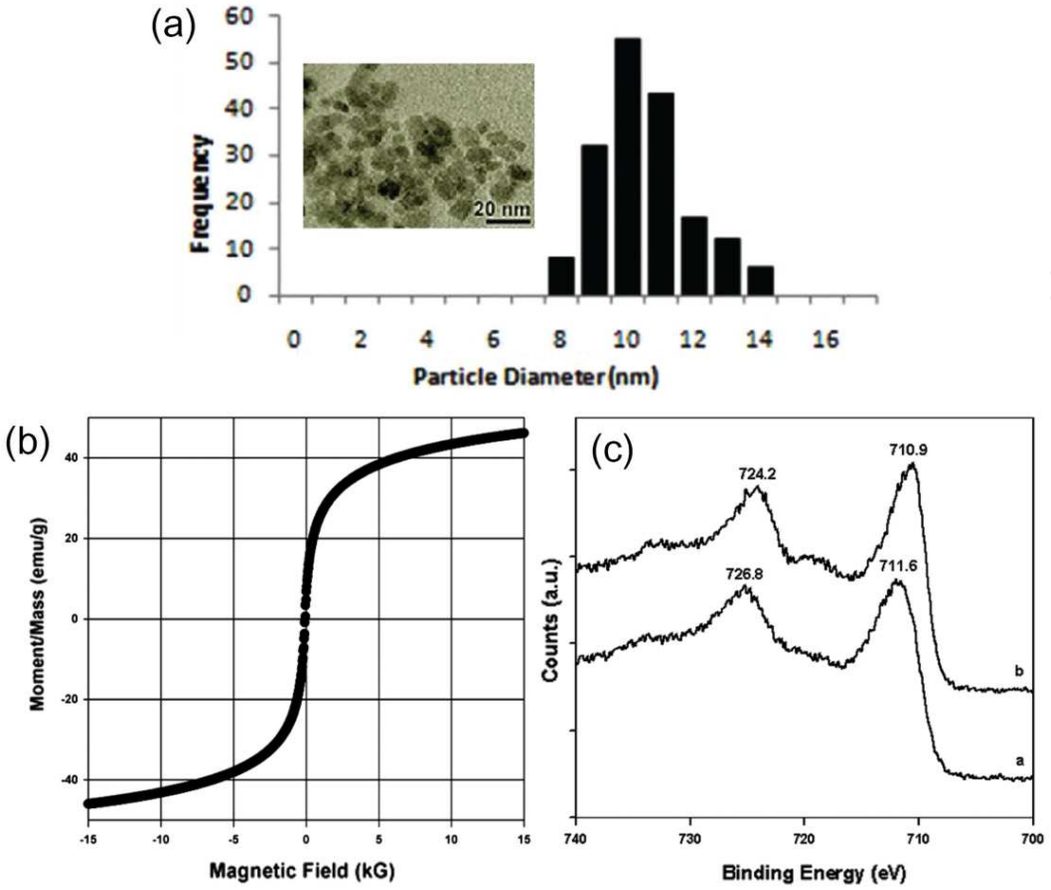

Figure 11. (a) Particle morphology, (b) superparamagnetic property, and (c) phase identification of the synthesized γ-Fe_2O_3 nanoparticles. Figure from [12].

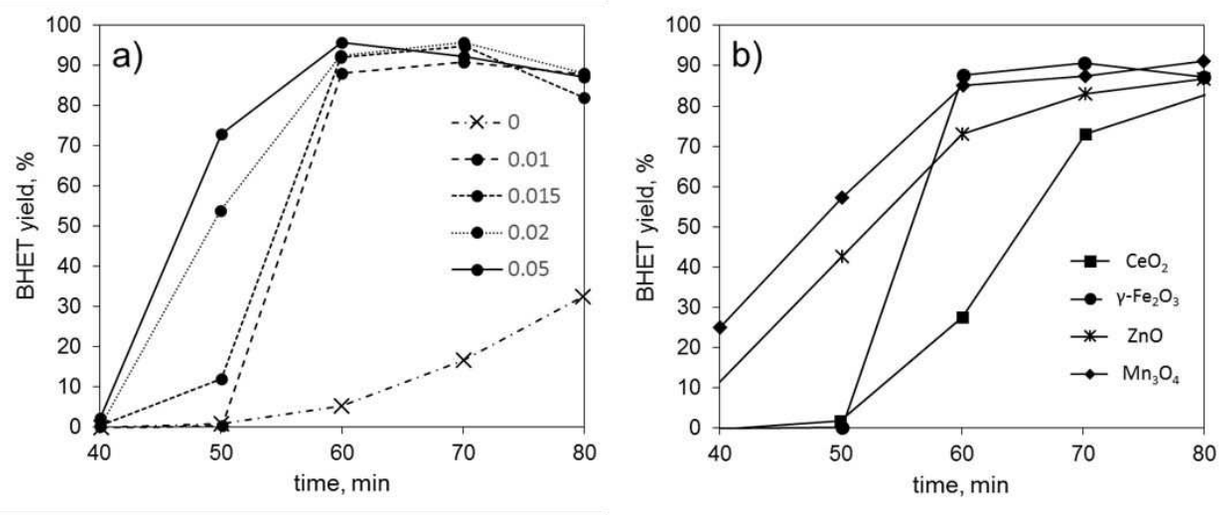

Figure 12. Catalytic performance of γ-Fe_2O_3 nanoparticles at various loadings and comparison to other metal oxide catalysts. Figure from [12].

The main potential of using γ-Fe_2O_3 as candidate for industrial glycolysis catalyst is the easy separation method and stability. In addition to the superparamagnetic property of γ-Fe_2O_3 nanoparticles that was beneficial to catalytic performance and separation, its stability with repeated use was also successfully demonstrated. The catalyst was reused in 10 reaction repeat cycles and did not significantly affect the BHET monomer yield, as shown in Figure 13. The thermal stability was supported by thermogravimetric analysis (TGA), while the XRD spectra of the used catalyst also proved phase stability [12]. These demonstrate the robust characteristics of the catalyst, withstanding repeated use at elevated temperature and pressure without deterioration in performance. Given comparable performance to a homogenous catalyst as shown in Figure 13b, the superparamagnetic catalyst provides a more practical approach to catalyst separation by application of a magnetic field.

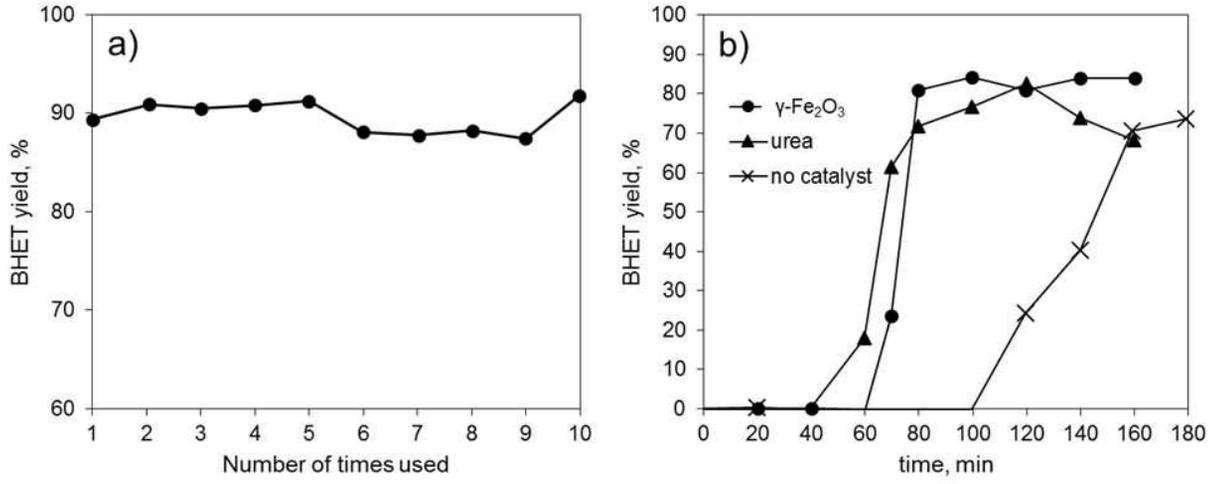

Figure 13. Assessment of catalyst stability with repeated use and comparison to a recoverable homogeneous catalyst at the same reaction conditions. Figure from [12].

2.4. Mesoporous spinel oxide catalysts

Due to several advantages such as high mechanical strength, possibility of regeneration, easier separation, and robust process integration, metal oxides can be considered superior to conventional PET glycolysis catalysts. Moreover, there are numerous possibilities to tailor their physical and chemical properties for the desired catalytic performance and functionality [47]. For the enhancement of catalytic activity, for example, altering the metal composition by introduction of another metal could result in higher catalytic activity [48–50]. The same principle is used to potentially enhance the performance of metal oxide catalysts for PET glycolysis. In this section, pure oxides and mixed-oxide spinel oxides of zinc, manganese, and cobalt were synthesised by simple precipitation or co-precipitation methods.

Simple precipitation method was used to synthesize the pure metal oxides. A 1.0 M solution of the salt precursors ($Mn(NO_3)_2$ xH_2O, $Zn(NO_3)_2$ $6H_2O$, or $Co(NO_3)_2$ $6H_2O$) was mixed with 0.1 M ammonium hydroxide to set the pH at 9.0. Precipitates of the corresponding metal

http://dx.doi.org/10.5772/62041

hydroxides formed, which were filtered, washed with water, and dried at 100°C for 8 h. The oxide form was obtained by calcination of the dried powder at 600°C for 4 h. For the mixed metal oxides, a modified co-precipitation method was implemented [51–53]. The molar ratios of the metal precursors were fixed to be 1:2. Similar to the previous synthesis, a 0.1 M ammonium hydroxide solution was stirred into the bimetallic precursor solutions, setting the pH value at 9.0. The same procedures for filtering, washing, drying, and calcining were performed on the mixed metal oxides [13]. The physical and chemical properties of the synthesized catalysts are summarized in Table 3. The analysis of atomic composition of the oxides via EDS was performed with results shown in Table 4.

Catalyst	BET surface area (m^2/g)	Pore volume (cm^3/g)	Average pore diameter (nm)	Acid site concentration (mmol/g)
ZnO	7.67	0.06	31.33	0.041
Co_3O_4	17.50	0.09	18.80	0.032
$ZnCo_2O_4$	21.65	0.08	12.23	0.045
Mn_3O_4	22.57	0.01	14.70	0.060
$CoMn_2O_4$	25.10	0.07	10.16	0.067
$ZnMn_2O_4$	32.40	0.14	14.50	0.088

Table 3. Surface area, pore dimensions, and acid site concentration of the pure and mixed oxide catalysts [53]

Catalyst	Atom percentage			Atomic ratio (Mixed oxides)			
Zn	Mn	Co	O	Mn/Zn	Mn/Co	Co/Zn	
ZnO	56.3	-	-	43.7	-	-	-
Mn_3O_4	-	61.4	-	38.6	-	-	-
Co_3O_4	-	-	75.9	24.1	-	-	-
$ZnMn_2O_4$	21.7	40.9	-	37.4	1.88	-	-
$CoMn_2O_4$	-	36.2	21.0	42.9	-	1.72	-
$ZnCo_2O_4$	24.1	-	38.9	37.0	-	-	1.61

Table 4. Atomic analysis of the synthesized oxide catalysts by EDX [53]

The catalytic activity of metal oxides in PET glycolysis is influenced by the interaction of the metal cation and the carbonyl oxygen in the polyester. The nature of the metal, oxidation state, and crystal structure affect this interaction. In spinel oxides, the metal cations can be located in tetrahedral and octahedral sites. The metal covalency of two or more different metals in the mixed oxides can result in a beneficial interaction that could enhance its redox properties and catalytic activity. In this study, the best catalytic activity for glycolysis was demonstrated by

$ZnMn_2O_4$ catalyst (Figure 14). This catalyst has the ion pair Zn^{2+}/Mn^{3+} in its crystal lattice compared to Co^{2+}/Mn^{3+} and Zn^{2+}/Co^{2+} in the other mixed spinels. The high activity of the catalyst was attributed to the nature of the manganese ions combined with structural effects in the spinel crystal [13].

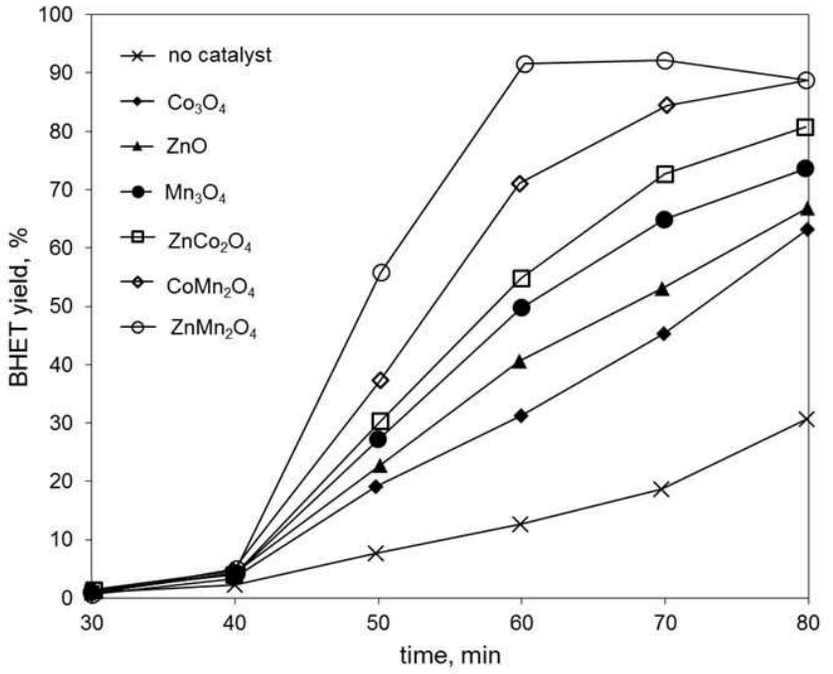

Figure 14. Comparison of BHET yields among the pure and mixed oxide catalysts [13].

2.5. Purity of recovered BHET monomer

For all the glycolysis reactions above using various catalysts, the recycled BHET was recovered via simple recrystallization. Several characterization methods have been employed to verify the structure and purity of the recovered monomer. The FT-IR spectra of the recycled BHET matched that of the standard sample [10], without extra peaks characteristic of contamination. As it is also possible that dimers and oligomers are not effectively separated, thermal and structure analyses have been performed using thermogravimetric analysis (TGA) and nuclear magnetic resonance spectroscopy (NMR). The proton and carbon NMR spectra identified peaks corresponding to distinct groups in the monomer and dimer backbones [13]. Along with TGA thermogram profiles, the structure characterization verified the good separation of the BHET from its oligomers.

3. Dopamine-induced carbon@silica hybrid as fuel cell anode catalyst

Aside from high proton conductivity and self-humidifying properties, principles of practical design for potential materials for polymer electrolyte membrane fuel cell (PEMFC) demand a

http://dx.doi.org/10.5772/62041

fabrication method that is non-toxic and requires no complex apparatus for easy and large-scale production. Hybrid catalysts with carbon material and inorganic material have received attention from many researchers for PEMFC [54,55].

In hybrid material synthesis, a variety of methods are used to combine organic and inorganic materials. However, these fabrication methods require expensive equipment and complex processes, thereby limiting mass production [56–58]. To resolve this problem, our group has developed a simple and green fabrication of a hybrid catalyst for PEMFC. The hybrid composite consists of Pt nanoparticle, conductive dopamine coating layer, and silica support. Pt nanoparticle has been used as a typical catalyst for electrode catalyst for energy storage application. We also used Pt nanoparticle as the anode catalyst for PEMFC. To deposit Pt nanoparticles on the surface of silica, we applied dopamine coating as an adhesive layer [9]. The overall synthesis procedure for the metal and dopamine-induced carbon@silica nanocomposite is illustrated in Figure 15.

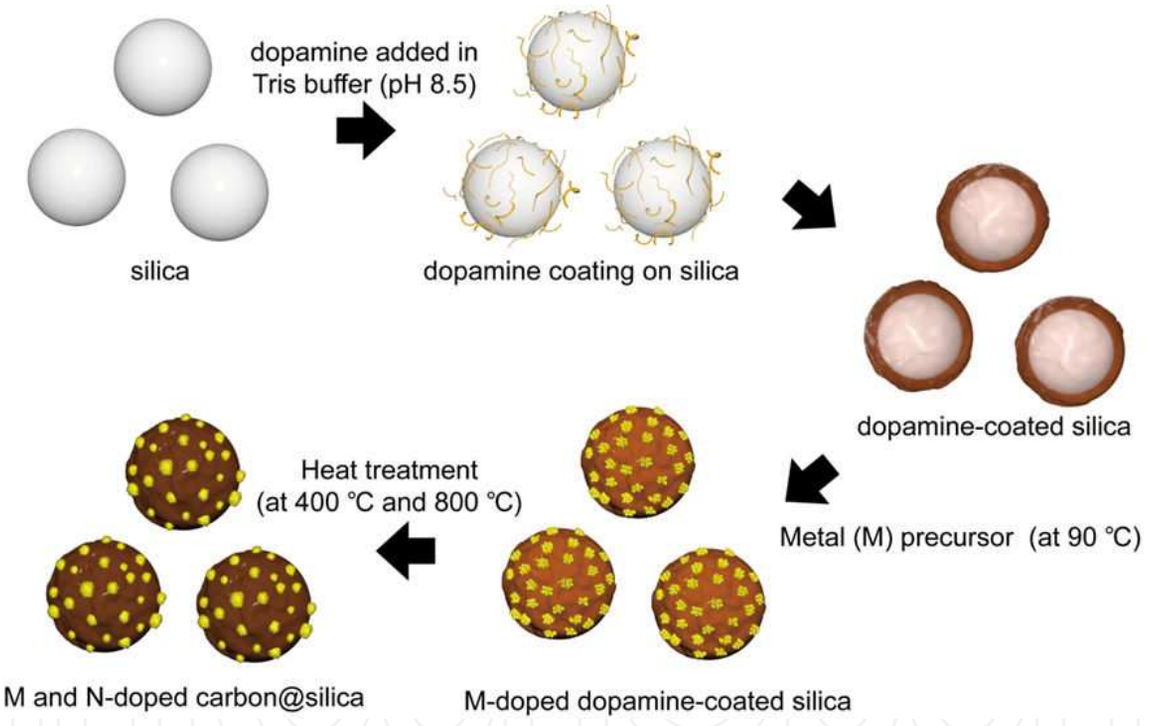

Figure 15. Overall procedure for synthesis of metal (M)- and nitrogen (N)-doped carbon@silica nanocomposite.

For the preparation of a hybrid anode catalyst, silica was fabricated by water-in-oil microemulsion method that produces a narrow size distribution. Silica is generally applied as support material because of its mechanical, chemical, and thermal stability. Its size and surface property can also be easily modified. Additionally, it has hygroscopic property that maintains the humidity needed for the proton conductivity in PEMFC. The humidity dependence of the membrane's conductivity typically required humidity control using an external equipment. However, the application of silica as support for the anode catalyst could provide both humidity and conductivity to the proton conductive membrane [8].

To deposit Pt nanoparticles on the surface of silica, we applied dopamine coating as an adhesive layer and self-reducing agent. Dopamine is a mussel-inspired adhesive based on a protein located at the end of the byssus of mussels. The protein allows mussels to strongly attach on rock surfaces or support in sea. The adhesion property of the protein helps mussels hold onto substrates in wet condition. Mussel-inspired dopamine is similar in chemical structure, with catechol and amine functional group as the protein [59]. Attempting to mimic the adhesive functionality, many researchers coated dopamine on various types of substrates. After dopamine coating, the substrate achieved a more hydrophilic surface and can be well dispersed in water. Dopamine coating also acts as a metal adhesive layer through the self-reducing ability of catechol group in the dopamine chemical structure [60]. Moreover, the coating is a simple and controllable dip-coating process in alkaline water solution (pH 8.5). The coating thickness can be tailored in nanoscale by adjusting the temperature, pH, time, and concentration of dopamine. Because of these advantages, dopamine coating has been applied to a variety of fields, such as surface modification, heavy metal removal, carbon material functionalization, and fabrication of conductive N-doped carbon sources [56–58,61].

We prepared Pt and N-doped carbon@silica with dopamine coating via metal decoration and carbonization steps. The dopamine coating procedure was performed on a Tris buffer solution at pH 8.5. Silica particles were dispersed in the solution. Then, 10 mM dopamine was added and mixed mildly for 6 h. After the coating step, the particle was washed several times with DI water. A thin layer of dopamine was observed to be coated well on silica with a thickness of 11.5 nm as shown in Figures 16c and 16d. The prepared dopamine-coated silica was re-dispersed in DI water. The dopamine-coated silica was then used to serve as catalyst support with metal adhesion properties. The Pt nanoparticles on the coated silica were deposited through the self-reducing ability of catechol groups in dopamine, as shown in Figure 17. This phenomenon releases electrons via the transformation of the R-OH group to a C=O group, which reduce Pt ions into Pt nanoparticles.

The dopamine coating layer naturally prohibits electron transfer (low conductivity). To enhance catalyst conductivity, we conducted carbonization of the Pt and dopamine-coated silica in an inert atmosphere at 800 °C. The carbonized dopamine layer contained nitrogen (N) and had other functional groups removed. N-doped carbon layer from dopamine coating enhanced both mechanical stability and conductivity of the material [57].

We applied Pt and dopamine-induced carbon@silica hybrid composite for polymer membrane electrolyte fuel cell as anode catalyst. The composite was evaluated and compared with commercial Pt/C catalyst under zero relative humidity. The carbonized dopamine coating and silica could be useful in PEMFC under non-humidified conditions. Pt and N-doped carbon@silica-based composites and commercial Pt/C were evaluated by galvanostatic polarization and power density curves as functions of current density for a single PEMFC at zero relative humidity (Figure 18). The Pt and dopamine-induced carbon@silica composite exhibited a maximum power density of 0.55 W cm^{-2}, which exceeds that of commercial Pt/C (0.45

http://dx.doi.org/10.5772/62041

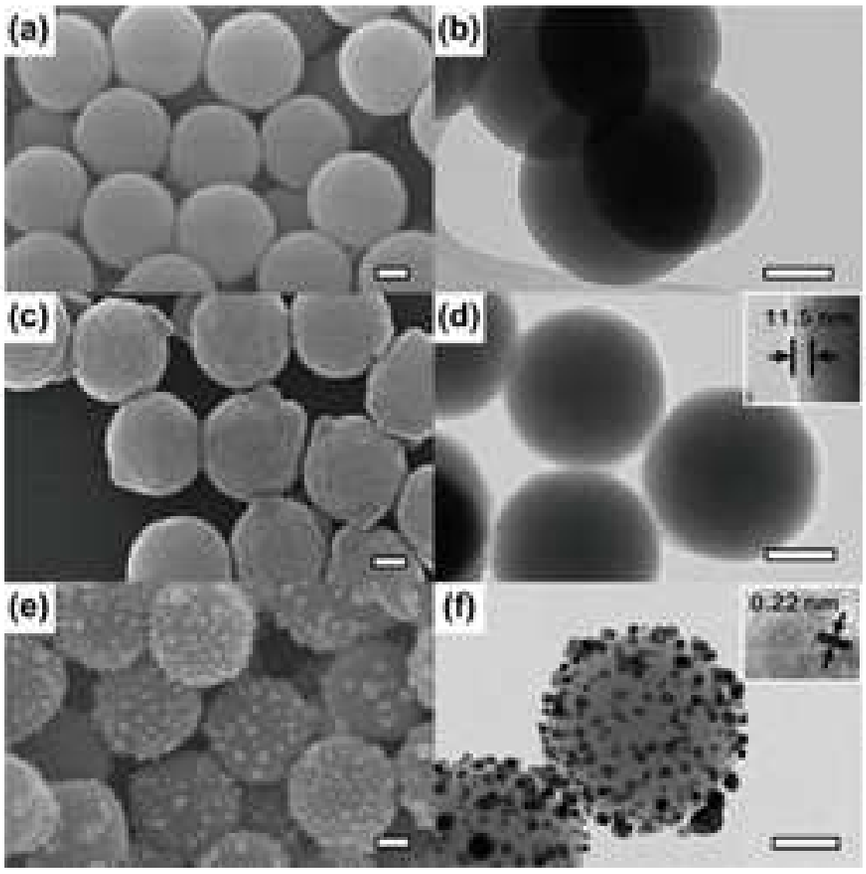

Figure 16. SEM and TEM images of (a and b) silica, (c and d) dopamine-coated silica, and (e and f) Pt and dopamine-induced carbon@silica. Scale bars are 100 nm.

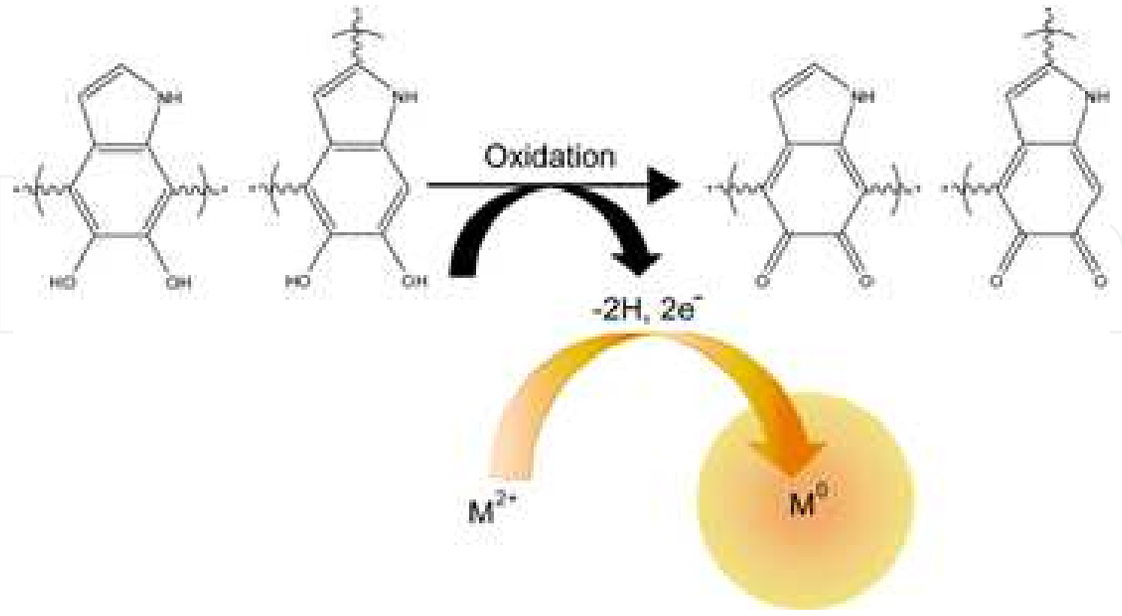

Figure 17. Reduction pathway from Pt ion into Pt nanoparticle using self-reducing ability of dopamine coating layer.

W cm^{-2}). The improved performance of the composite is attributed to the hybrid synergy effect of silica hygroscopic property and N-doped dopamine-induced carbon layer. Additionally, the N-doped carbon obtained after the carbonization step could make the composite more conductive with the enhancement of charge transfer at interfaces. As a result, these advantages of the Pt and dopamine-induced carbon@silica composite could contribute to enhance performance under low humidity conditions compared to the commercial Pt/C catalyst.

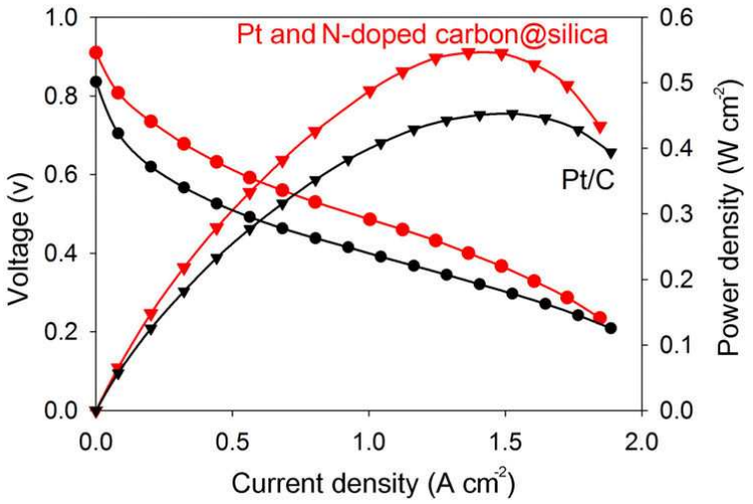

Figure 18. I-V polarization (left axis) and power density (right axis) curve for PEMFC single cell (H_2/O_2) with Pt and N-doped carbon@silica nanocomposites (red triangle) and commercial Pt/carbon (black circle) used as an anode catalyst under relative humidity at 0%.

4. Conclusion

We have presented various techniques to obtain novel catalysts that successfully enhance the efficiency and productivity of PET glycolysis for monomer recycling as well as the performance of polymer electrolyte membrane fuel cells. The catalysts can be considered a practical solution that addresses various issues in these processes, such as catalyst separability, reusability, and performance in limited operating conditions. The use of ultrasound-assisted synthesis provided an efficient alternative synthesis approach to obtain metal-oxide composites of silica and graphene oxide under mild conditions. The use of these catalyst composites offers the potential of industrial-scale use given their high activity in addition to thermal and chemical stability. Another practical and effective approach is the use of a magnetically recoverable catalyst, γ-Fe_2O_3. The superparamagnetic nanocatalyst, offering comparable performance and stability as the other solid catalysts, has further advantages of efficient separation and relatively simplicity of synthesis approach. For fuel cell development, we developed a non-toxic and easy chemical method to fabricate Pt and dopamine-induced carbon@silica composite without complex apparatus. The silica nanoparticles as support material acted as a self-humidifying material, while the dopamine coating played the role of a self-reducing agent and adhesive layer for anchoring the Pt nanoparticles. Additionally, the N-doped carbon from

carbonization of dopamine coating enhanced electrical conductivity of the composite. This resulted to overall superior performance of the composite as anode catalyst even under low humidity conditions. The fabrication methods and alternative catalysis strategies presented will be valuable for the commercialization of green catalysts for PET monomer recycling and energy conversion systems.

Acknowledgements

This work was supported by the R&D Center for Valuable Recycling (Global-Top Environmental Technology Development Program) funded by the Ministry of Environment (Project No.: GT-11-C-01-250-0) and by Basic Science Research Program through the National Research Foundation of Korea (NRF) funded by the Ministry of Science, ICT & Future Planning (No. 2014R1A5A1009799).

Author details

Arvin Sangalang, Seunghwan Seok and Do Hyun Kim*

*Address all correspondence to: DoHyun.Kim@kaist.ac.kr

Department of Chemical and Biomolecular Engineering, KAIST, Daejeon, Republic of Korea

References

[1] Smithers P. Demand for PET packaging material in 2019 [Internet]. April 2014. Available from: http://www.smitherspira.com/news/2014/april/demand-for-pet-packaging-material-in-2019 [Accessed: 2015-10-03]

[2] Scheirs J, Long TE, editors. Modern Polyesters: Chemistry and Technology of Polyesters and Copolyesters. England: John Wiley & Sons Ltd; 2003. 750 p.

[3] Welle F. Twenty years of PET bottle to bottle recycling. Resources Conserv. Recycling. 2011;55(11):865–875. DOI: 10.1016/j.resconrec.2011.04.009

[4] Shen L, Worrell E, Patel MK. Open-loop recycling: a LCA case study of PET bottle-to-fibre recycling. Resources Conserv. Recycling. 2010;55(1):34–52. DOI: 10.1016/j.resconrec.2010.06.014

[5] Bartolome L, Imran M, Cho BG, Al-Masry WA, Kim DH. Recent developments in the chemical recycling of PET. In: Achilias D, editor. Material Recycling — Trends and Perspectives. INTECH; 2012. p. 65–84. DOI: 10.5772/33800

[6] George N, Kurian T. Recent developments in the chemical recycling of postconsumer poly(ethylene terephthalate) melts. Ind. Eng. Chem. 2014;53(37):14185–14198. DOI: 10.1021/ie501995m

[7] Lorenzetti C, Manaresi P, Berti C, Barbiroli G. Chemical recovery of useful chemicals from polyester (PET) waste for resource conservation: a survey of state of the art. J. Polym. Environ. 2006;14(1):89–101. DOI: 10.1007/s10924-005-8711-1

[8] Choi I, Lee KG, Ahn SH, Kim DH, Kwon OJ, Kim JJ. Sonochemical synthesis of Pt-deposited SiO_2 nanocomposite and its catalytic application for polymer electrolyte membrane fuel cell under low-humidity conditions. Catal. Commun. 2012;21:86–90. DOI: 10.1016/j.catcom.2012.02.005

[9] Seok S, Choi I, Lee KG, Choi BG, Park KJ, Park JY, Kwon OJ, Lee SJ, Kim DH. Dopamine-induced Pt and N-doped carbon@silica hybrids as a high-performance anode catalyst of polymer electrolyte membrane fuel cell. RSC Adv. 2014;4:42582–42584. DOI: 10.1039/C4RA06819J

[10] Imran M, Lee KG, Imtiaz Q, Kim BG, Han M, Kim DH. Metal oxide-doped silica nanoparticles for the catalytic glycolysis of polyethylene terephthalate. J. Nanosci. Nanotechnol. 2011;11(1):824–828. DOI: 10.1166/jnn.2011.3201

[11] Park G, Bartolome L, Lee KG, Lee SJ, Kim DH, Park TJ. One-step sonochemical synthesis of a graphene oxide-manganese oxide nanocomposite for catalytic glycolysis of poly(ethylene terephthalate). Nanoscale. 2012;4(13):3879–3885. DOI: 10.1039/C2NR30168G

[12] Bartolome L, Imran M, Lee KG, Sangalang A, Ahn JK, Kim DH. Superparamagnetic γ-Fe_2O_3 nanoparticles as easily recoverable catalyst for the chemical recycling of PET. Green Chem. 2014;16(1):279–286. DOI: 10.1039/C3GC41834K

[13] Imran M, Kim DH, Al-Masry WA, Mahmood A, Hassan A, Haider S, Ramay SM. Manganese-, cobalt-, and zinc-based mixed-oxide spinels as novel catalysts for the chemical recycling of poly(ethylene terephthalate) via glycolysis. Polym. Degrad. Stabil. 2013;98(4):904–915. DOI: 10.1016/j.polymdegradstab.2013.01.007

[14] Min BK, Santra AK, Goodman DW. Understanding silica-supported metal catalysts: Pd/silica as a case study. Catal. Today. 2003;85(2):113–124. DOI: 10.1016/S0920-5861(03)00380-8

[15] Juszczyk W, Karpiński Z. Characterization of supported palladium catalysts; II. $PdSiO_2$. J. Catal. 1989;117(2):519–532. DOI: 10.1016/0021-9517(89)90361-8

[16] Xie Z, Liu Z, Wang Y, Yang Q, Xu L, Ding W. An overview of recent development in composite catalysts from porous materials for various reactions and processes. Int. J. Mol. Sci. 2010;11(5):2152–2187. DOI: 10.3390/ijms11052152

[17] Stankovich S, Dikin DA, Dommett GHB, Kohlhaas KM, Zimney EJ, Stach EA, Piner RD, Nguyen ST, Ruoff RS. Graphene-based composite materials. Nature. 2006;442(7100):282–286. DOI: 10.1038/nature04969

[18] Stankovich S, Piner RD, Nguyen ST, Ruoff RS. Synthesis and exfoliation of isocyanate-treated graphene oxide nanoplatelets. Carbon. 2006;44(15):3342–3347. DOI: 10.1016/j.carbon.2006.06.004

[19] Muszynski R, Seger B, Kamat PV. Decorating graphene sheets with gold nanoparticles. J. Phys. Chem. C. 2008;112(14):5263–5266. DOI: 10.1021/jp800977b

[20] Bai H, Li C, Wang X, Shi G. A pH-sensitive graphene oxide composite hydrogel. Chem. Commun. 2010;46(14):2376–2378. DOI: 10.1039/C000051E

[21] Suslick KS, Price GJ. Applications of ultrasound to materials chemistry. Annu. Rev. Mater. Sci. 1999;29(1):295–326. DOI: 10.1146/annurev.matsci.29.1.295

[22] Okitsu K, Bandow H, Maeda Y. Sonochemical preparation of ultrafine palladium particles. Chem. Mater. 1996;8(2):315–317. DOI: 10.1021/cm950285s

[23] Park G, Lee KG, Lee SJ, Park TJ, Wi R, Kim DH. Synthesis of graphene-gold nanocomposites via sonochemical reduction. J. Nanosci. Nanotechnol. 2011;11(7):6095–6101. DOI: 10.1166/jnn.2011.4446

[24] Lee KG, Wi R, Park TJ, Yoon SH, Lee J, Lee SJ, Kim DH. Synthesis and characterization of gold-deposited red, green and blue fluorescent silica nanoparticles for biosensor application. Chem. Commun. 2010;46(34):6374–6376. DOI: 10.1039/C0CC00762E

[25] Doktycz SJ, Suslick KS. Interparticle collisions driven by ultrasound. Science. 1990;247:1067–1069. DOI: 10.1126/science.2309118

[26] Suslick KS. Sonochemistry. Science. 1990;247:1439–1445. DOI: 10.1126/science.247.4949.1439

[27] Wang H, Cui LF, Yang Y, Casalongue HS, Robinson JT, Liang Y, Cui Y, Dai H. Mn_3O_4-graphene hybrid as a high-capacity anode material for lithium ion batteries. J. Am. Chem. Soc. 2010;132(40):13978–13980. DOI: 10.1021/ja105296a

[28] Yan J, Fan Z, Wei T, Qian W, Zhang M, Wei F. Fast and reversible surface redox reaction of graphene-MnO_2 composites as supercapacitor electrodes. Carbon. 2010;48(13):3825–3833. DOI: 10.1016/j.carbon.2010.06.047

[29] Chen S, Zhu J, Wang X. From graphene to metal oxide nanolamellas: a phenomenon of morphology transmission. ACS Nano. 2010;4(10):6212–6218. DOI: 10.1021/nn101857y

[30] Yin J, Gao F, Wu Y, Wang J, Lu Q. Synthesis of Mn_3O_4 octahedrons and other manganese-based nanostructures through a simple and green route. CrystEngComm. 2010;12(11):3401–3403. DOI: 10.1039/C003551N

[31] Liu B, Thomas PS, Williams RP, Donne SW. Thermal characterisation of chemically reduced electrolytic manganese dioxide. J. Thermal Anal. Calorim. 2005;80(3):625–629. DOI: 10.1007/s10973-005-0704-8

[32] Huang H, Wang X. Graphene nanoplate-MnO_2 composites for supercapacitors: a controllable oxidation approach. Nanoscale. 2011;3(8):3185–3191. DOI: 10.1039/C1NR10229J

[33] Qiu LG, Li ZQ, Wu Y, Wang W, Xu T, Jiang X. Facile synthesis of nanocrystals of a microporous metal-organic framework by an ultrasonic method and selective sensing of organoamines. Chem. Commun. 2008;31:3642–3644. DOI: 10.1039/B804126A

[34] Offeman RE, Hummers WS. Preparation of graphitic oxide. J. Am. Chem. Soc. 1958;80:1339.

[35] López-Fonseca R, Duque-Ingunza I, De Rivas B, Arnaiz S, Gutiérrez-Ortiz JI. Chemical recycling of post-consumer PET wastes by glycolysis in the presence of metal salts. Polym. Degrad. Stabil. 2010;95(6):1022–1028. DOI: 10.1016/j.polymdegradstab.2010.03.007

[36] Wang H, Li Z, Liu Y, Zhang X, Zhang S. Degradation of poly (ethylene terephthalate) using ionic liquids. Green Chem. 2009;11(10):1568–1575. DOI: 10.1039/B906831G

[37] Wang H, Liu Y, Li Z, Zhang X, Zhang S, Zhang Y. Glycolysis of poly (ethylene terephthalate) catalyzed by ionic liquids. Eur. Polym. J. 2009;45(5):1535–1544. DOI: 10.1016/j.eurpolymj.2009.01.025

[38] Wang H, Yan R, Li Z, Zhang X, Zhang S. Fe-containing magnetic ionic liquid as an effective catalyst for the glycolysis of poly (ethylene terephthalate). Catal. Commun. 2010;11(8):763–767. DOI: 10.1016/j.catcom.2010.02.011

[39] Yue QF, Wang CX, Zhang LN, Ni Y, Jin YX. Glycolysis of poly (ethylene terephthalate) (PET) using basic ionic liquids as catalysts. Polym. Degrad. Stabil. 2011;96(4):399–403. DOI: 10.1016/j.polymdegradstab.2010.12.020

[40] Wi R, Imran M, Lee KG, Yoon SH, Cho BG, Kim DH. Effect of support size on the catalytic activity of metal-oxide-doped silica particles in the glycolysis of polyethylene terephthalate. J. Nanosci. Nanotechnol. 2011;11(7):6544–6549. DOI: 10.1166/jnn.2011.4393

[41] Wang Q, Yao X, Tang S, Lu X, Zhang X, Zhang S. Urea as an efficient and reusable catalyst for the glycolysis of poly (ethylene terephthalate) wastes and the role of hydrogen bond in this process. Green Chem. 2012;14(9):2559–2566. DOI: 10.1039/C2GC35696A

[42] Koukabi N, Kolvari E, Khazaei A, Zolfigol MA, Shirmardi-Shaghasemi B, and Khavasi HR. Hantzsch reaction on free nano-Fe_2O_3 catalyst: excellent reactivity combined with facile catalyst recovery and recyclability. Chem. Commun. 2011;47(32):9230–9232. DOI: 10.1039/C1CC12693H

[43] Garade AC, Bharadwaj M, Bhagwat SV, Athawale AA, Rode CV. An efficient γ-Fe_2O_3 catalyst for liquid phase air oxidation of p-hydroxybenzyl alcohol under mild conditions. Catal. Commun. 2009;10(5):485–489. DOI: 10.1016/j.catcom.2008.10.044

[44] Picasso G, Quintilla A, Pina MP, Herguido J. Total combustion of methyl-ethyl ketone over Fe_2O_3 based catalytic membrane reactors. Appl. Catal. B: Environ. 2003;46(1):133–143. DOI: 10.1016/S0926-3373(03)00219-4

[45] Kang YS, Risbud S, Rabolt JF, Stroeve P. Synthesis and characterization of nanometer-size Fe_3O_4 and γ-Fe_2O_3 particles. Chem. Mater. 1996;8(9):2209–2211. DOI: 10.1021/cm960157j

[46] Jeong, JR, Lee SJ, Kim JD, Shin SC. Magnetic properties of γ-Fe_2O_3 nanoparticles made by coprecipitation method. Phys. Stat. Solidi B Basic Res. 2004;241(7):1593–1596. DOI: 10.1002/pssb.200304549

[47] Henry CR. Catalysis by nanoparticles. In: Heiz U, Landman U, editors. Nanocatalysis. Heidelberg: Springer Berlin/Heidelberg; 2007. p. 245–268. DOI: 10.1007/978-3-540-32646-5

[48] Ghose J, Murthy K. Activity of Cu^{2+} ions on the tetrahedral and octahedral sites of spinel oxide catalysts for CO oxidation. J. Catal. 1996;162(2):359–360. DOI: 10.1006/jcat.1996.0293

[49] Guilhaume N, Primet M. Catalytic combustion of methane: copper oxide supported on high-specific-area spinels synthesized by a sol-gel process. J. Chem. Soc. Faraday Trans. 1994;90(11):1541–1545. DOI: 10.1039/FT9949001541

[50] Słoczyński J, Ziółkowski J, Grzybowska B, Grabowski R, Jachewicz D, Wcisło K, Gengembre L. Oxidative dehydrogenation of propane on $Ni_xMg_{(1-x)}Al_2O_4$ and $NiCr_2O_4$ spinels. J. Catal. 1999;187(2):410–418. DOI: 10.1006/jcat.1999.2626

[51] Niu X, Du W, Du W. Preparation and gas sensing properties of ZnM2O4 (M=Fe, Co, Cr). Sens. Actuators B: Chem. 2004;99(2):405–409. DOI: 10.1016/j.snb.2003.12.007

[52] Ferraris G, Fierro G, Jacono ML, Inversi M, Dragone R. A study of the catalytic activity of cobalt-zinc manganites for the reduction of NO by hydrocarbons. Appl. Catal. B: Environ. 2002;36(4):251–260. DOI: 10.1016/S0926-3373(01)00289-2

[53] Mokhtar M, Basahel SN, Al-Angary YO. Nanosized spinel oxide catalysts for CO-oxidation prepared via CoMnMgAl quaternary hydrotalcite route. J. Alloys Compounds. 2010;493(1):376–384. DOI: 10.1016/j.jallcom.2009.12.106

[54] Zhang L, Wang L, Holt CMB, Zahiri B, Li Z, Malek K, Navessin T, Eikerling MH, Mitlin D. Highly corrosion resistant platinum-niobium oxide-carbon nanotube electrodes for the oxygen reduction in PEM fuel cells. Energy Environ. Sci. 2012;5(3):6156–6172. DOI: 10.1039/C2EE02689A

[55] Long D, Li W, Qiao W, Miyawaki J, Yoon SH, Mochida I, Ling L. Partially unzipped carbon nanotubes as a superior catalyst support for PEM fuel cells. Chem. Commun. 2011;47(33):9429–9431. DOI: 10.1039/C1CC13488D

[56] Hong D, You I, Lee H, Lee S-G, Choi IS, Kang SM. Polydopamine circle-patterns on a superhydrophobic AAO surface: water-capturing property. Bull. Kor. Chem. Soc. 2013;34(10):3141–3142. DOI: 10.5012/bkcs.2013.34.10.3141

[57] Ryu S, Chou JB, Lee K, Lee D, Hong SH, Zhao R, Lee H, Kim SG. Direct insulation-to-conduction transformation of adhesive catecholamine for simultaneous increases of electrical conductivity and mechanical strength of CNT fibers. Adv. Mater. 2015;27(21):3250–3255. DOI: 10.1002/adma.201500914

[58] Lee M, Rho J, Lee D-E, Hong S, Choi SJ, Messersmith PB, Lee H. Water detoxification by a substrate-bound catecholamine adsorbent. ChemPlusChem. 2012;77(11):987–990. DOI: 10.1002/cplu.201200209

[59] Lee H, Dellatore SM, Miller WM, Messersmith PB. Mussel-inspired surface chemistry for multifunctional coatings. Science. 2007;318(5849):426–430. DOI: 10.1126/science.1147241

[60] Hong S, Lee JS, Ryu J, Lee SH, Lee DY, Kim D-P, Park CB, Lee H. Bio-inspired strategy for on-surface synthesis of silver nanoparticles for metal/organic hybrid nanomaterials and LDI-MS substrates. Nanotechnology. 2011;22(49):494020. DOI: 10.1088/0957-4484/22/49/494020

[61] Kang SM, Park S, Kim D, Ruoff RS, Lee H. Simultaneous reduction and surface functionalization of graphene oxide by mussel-inspired chemistry. Adv. Funct. Mater. 2011;21(1):108–112. DOI: 10.1002/adfm.201001692